ORIGINAL PAPER

Activation of the cisplatin and transplatin complexes in solution with constant pH and concentration of chloride anions; quantum chemical study

Tomáš Zimmermann · Jerzy Leszczynski ·
Jaroslav V. Burda

Abstract The thermodynamics of cisplatin and transplatin hydration is studied within the model of constant pH solution. Several implicit solvation models were chosen for the determination of pK_a and pK constants of the hydration reactions. The polarizable dielectric model (DPCM), integral equation formalism polarizable model (IEFPCM), and polarizable conductor model (CPCM) were combined with the 'united atom model for Hartree-Fock' (UAHF) method for cavity construction and the B3LYP/6-31++G(2dp,2pd) level of calculations for the determination of electronic energies. The results were compared with the COSMO-RS and SM8 model developed by Truhlar (with M06 and MPWX functionals and the charge model CM4). The RMS difference between experimental and calculated pK_a values of cis/transplatin, water, HCl, and NH_4^+ was used to evaluate accuracy of calculations. The DPCM model was confirmed to perform the best. The predicted pK_a constants were used in Legendre transformation for the estimation of the $\Delta G'$ energies in the constant-pH model. The dependence of the pK constant on pH is plotted and compared with experimental value at pH=7.4. The influence of various chloride concentration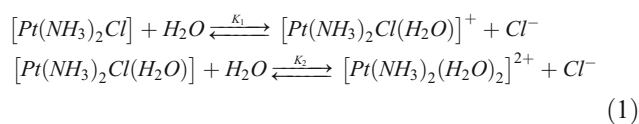s on the molar fractions of dissolved forms of cisplatin is examined for the DPCM model. The increased ratio of cisplatin active aqua-forms is clearly visible for 4 mM chloride solution in comparison with 104 mM Cl^- concentration.

Introduction

In this study, the hydration process of cis-dichloro-diammine-platinum, one of the most potent metallodrug, is explored in the models with constant pH and pCl values.

When cisplatin reach the cellular environment, the concentration of Cl^- anions drops from ca 100 mM (in blood stream) to the 4–80 mM depending on the type of the cell. In a solution with such a low Cl^- concentration, the process of cisplatin activation is facilitated. The activation process is connected with relatively simple substitution reaction where Cl ligand(s) in Pt(II) complex is/are released and replaced by water molecule(s). These hydration processes were experimentally studied in many laboratories. One of the first published works in this field comes from Hindmarch et al. [1] who performed the measurements for the replacement of both chloro ligands according to chemical reactions:
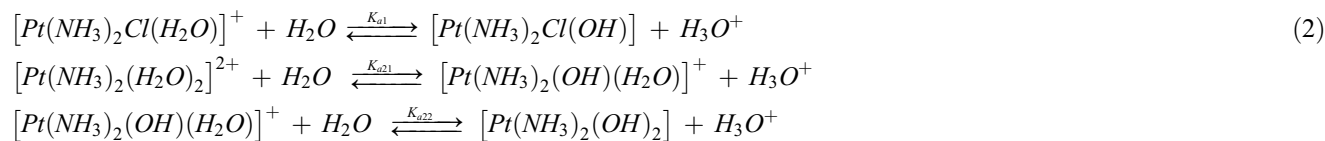
$$\left[Pt(NH_3)_2Cl\right] + H_2O \underset{}{\overset{K_1}{\rightleftarrows}} \left[Pt(NH_3)_2Cl(H_2O)\right]^+ + Cl^-$$
$$\left[Pt(NH_3)_2Cl(H_2O)\right] + H_2O \underset{}{\overset{K_2}{\rightleftarrows}} \left[Pt(NH_3)_2(H_2O)_2\right]^{2+} + Cl^-$$

(1)

These experiments were done in 1.0 M solution of $NaClO_4$ and they determined the equilibrium constants: log K_1 =- 2.19 and log K=- 3.53. Analogous processes for transplatin complex were explored in the more dilute

T. Zimmermann · J. V. Burda (✉)
Department of Chemical Physics and Optics,
Faculty of Mathematics and Physics, Charles University,
Ke Karlovu 3,
121 16, Prague 2, Czech Republic
e-mail: burda@karlov.mff.cuni.cz

J. Leszczynski
Department of Chemistry and Biochemistry,
Jackson State University,
1325 J.R. Lynch Street,
Jackson, MS 39217–0510, USA

(0.1 M) NaClO$_4$ solution by Arpalahti et al. [2, 3]. They revealed log K$_1$=- 2.92 and log K$_2$=- 4.41. In both cases the pH of the solution was 7.4.

It is known that the hydrated complexes can be stabilized in solutions with higher pH due to the proton release which turns the aqua ligand(s) into hydroxo ligand(s) [4]. In such solutions (pH>8), the hydrated cisplatin become not activated but actually passivated due to the formation of the more stable dihydoxo- platinum(II) complex:

$$\left[Pt(NH_3)_2Cl(H_2O)\right]^+ + H_2O \xrightleftharpoons{K_{a1}} \left[Pt(NH_3)_2Cl(OH)\right] + H_3O^+$$

$$\left[Pt(NH_3)_2(H_2O)_2\right]^{2+} + H_2O \xrightleftharpoons{K_{a21}} \left[Pt(NH_3)_2(OH)(H_2O)\right]^+ + H_3O^+$$

$$\left[Pt(NH_3)_2(OH)(H_2O)\right]^+ + H_2O \xrightleftharpoons{K_{a22}} \left[Pt(NH_3)_2(OH)_2\right] + H_3O^+ \tag{2}$$

Corresponding pK_a values for both cisplatin and transplatin complexes were determined in several laboratories, e.g., ref. [5–8]. Generally accepted (averaged) values for cisplatin are: pK$_{a1}$=6.6, pK$_{a21}$=5.5, and pK$_{a22}$=7.3. In the case of transplatin the values: pK$_{a1}$=5.6, pK$_{a21}$=4.4, and pK$_{a22}$=7.3 can be found in literature [9]. It can be noticed that transplatin deprotonates more readily, in lower pH, than cisplatin.

Besides the thermodynamic parameters, the reaction kinetics of these hydration processes was examined. It is known [10] that similar substitution reactions of transition metals often occur by association mechanism. The mechanism is however dependent on the type of individual ligands, e.g., the work of Chval [11] and some references in this paper. For these kinds of ligands which do not have the possibility of π-interaction (back-donation), a steric hindrance of more bulky substituents can slow down the reaction course but the change to dissociative mechanism is not probable [12]. Nevertheless, in several papers we have shown that this hydration reaction should be considered as a pseudo-dissociative since exchanging ligands are only very weakly bonded in TS structures [13].

While the forward reaction can be regarded as a pseudo first order kinetic reaction the backward reaction follows the second order reaction description. Experimentally determined rate constants are collected in Table 1 for temperature T=318.2 K, pH in range of 2.8-3.4 and 0.1 M NaClO$_4$ solution.

In a similar way, the rate constants for interaction of cisplatin with guanine were determined. In these studies, the hydration process of cisplatin coordinated to guanine (k_3) was examined as well as the replacement of the first and/or second aqua ligand by guanine (k_{P1} and k_{P2}):

$$cis - \left[Pt(NH_3)_2Cl(N7-Gua)\right]^+ + H_2O \xrightleftharpoons{k_3}$$
$$cis - \left[Pt(NH_3)_2(H_2O)(N7-Gua)\right]^{2+} + Cl^-$$
$$cis - \left[Pt(NH_3)_2Cl(H_2O)\right]^+ + Gua \xrightleftharpoons{k_{P1}}$$
$$cis - \left[Pt(NH_3)_2Cl(N7-Gua))\right]^+ + H_2O$$
$$cis - \left[Pt(NH_3)_2(H_2O)_2\right]^{2+} + Gua \xrightleftharpoons{k_{P2}}$$
$$cis - \left[Pt(NH_3)_2(H_2O)(N7-Gua)\right]^{2+} + H_2O \tag{3}$$

Based on several experimental works (see ref. [5, 14–20]) these rate constants can be estimated as follows: $k_3 = 7.6 \times 10^{-5} [s^{-1}]$, $k_{P1} = 1.5 \times 10^{-4}$ and $k_{P2} = 92 [M^{-1}s^{-1}]$ (for averaged concentration of Pt(II) complex ca 5 μM and guanine concentration about 0.8 mM). From these values it is apparent that the k_3 is comparable with corresponding k_1 and k_2 rate constants from Table 1. However, the values of k_{P1} and k_{P2} clearly show that guanine will interact substantially faster (about 5 orders of magnitude) with diaqua platinum complex (fully hydrated one) than with monoaqua-platinum complex. From these results the important role of the activation process, especially formation of fully hydrated cisplatin is apparent.

As for the computational approach, a lot of studies were performed recently on the topic of the cisplatin hydration. Besides several papers [21–24] from our laboratory, many other groups contributed to this area, too. The aquation process of the Pt(II) complexes was also examined by Zhang et al.[25], who used several DFT functionals combined with the PCM implicit solvation model. Despite some differences in theoretical models, qualitative agreement with our results was obtained. Robertazzi et al. [26] used an explicit solvation of cisplatin and compared the optimized structures with

Table 1 Rate constants of the hydration reaction of cis-/transplatin in the first and second stage (cf. Eq. 1)

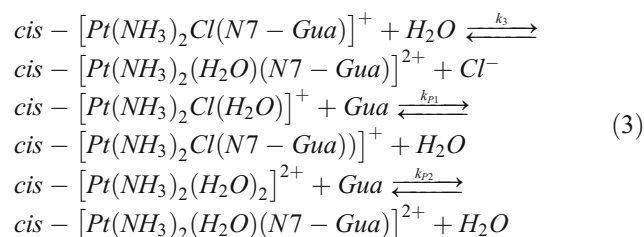|	Cisplatin[a]	Transplatin[b]
k$_1$ [s^{-1}]	(1.9±0.2)×10^{-4}	(1.05±0.03)×10^{-3}
k$_{-1}$ [M^{-1}s^{-1}]	(6.0±1.5)×10^{-2}	2.2±0.4
k$_2$ [s^{-1}]	(2.3±0.3)×10^{-4}	(4±2)×10^{-6}
k$_{-2}$ [M^{-1}s^{-1}]	(9.9±1.4)×10^{-1}	(2.0±0.2)×10^{-1}

[a] Ref. [2]

[b] Ref. [3]

the gas phase results showing a few kcal mol^{-1} lowering of activation barrier in solvent. Another calculations devoted to the hydration of the Pt(II) complexes were published by Dos Santos group [27, 28]. The authors gave a thorough insight on the effect of various contributions in multipole expansion of the self-consistent reaction field method. Even though they focused on dechlorination of the Pt(II)-ethylenediammine complex, resulting hydration characteristics are very close to those for cisplatin. This illustrates the reliability of the computational approaches since there is a close relationship between the cisplatin and Pt(en)Cl$_2$ complexes. Recently, a series of papers on platinum(II) complexes was published by this group [29–31] where several other aspects are discussed in detail. Chojnacki et al. [32] made another attempt to elucidate the hydration process of cisplatin and transplatin in both the gas phase and PCM approach. The same Pt(II) complexes were also examined using the classical MD and explicit water solvation model [33].

Lately, several new studies on hydration of other platinum drugs appeared. Banerjee et al. [34] investigated the AMD443 anticancer drug using the DFT method and implicit solvation model. The mechanism of hydrolytic reactions of carboplatin and oxaliplatin was explored by Pavelka et al. [35, 36] using B3LYP combined with the PCM model. Activation barriers they obtained were a little bit too high compared with the experimental data. Another study on hydration of the EDO complex of ethyldiamine-oxalatoplatinum(II) was published recently [37]. Also, comparison of the general square-planar Pt(II) compounds was presented by Dans et al. [38].

In the following sections the importance of the correct environmental model on the thermodynamic description of the hydrolytic process based on chemical reaction in Eq. 1 will be demonstrated. For this purpose the Legendre transformation of the standard reaction Gibbs free energy will be performed in order to obtain the appropriate thermodynamic potential with pH as a natural variable.

Computational details

All the optimizations were performed at the B3LYP/ 6-31++G(d,p) level with IEFPCM model [39] and the UAHF cavity [40]. Stuttgart's ECP: MWB-60 [41] and MWB-10 [42] were used for the description of the core electrons of the Pt and Cl atoms with the extension of original pseudoorbitals as discussed in our previous papers [21, 23]. Since we focus only on the thermodynamic description, all reactant and product components were considered as isolated species. Frequency analysis was used to confirm

the minimum character of each geometry and for the determination of the thermal and entropy corrections to the Gibbs free energy based on the canonical ensemble of statistical physics. For the optimized geometries, single-point energies were determined at the B3LYP/6-311++G (2df,2pd) level with the same ECP and with augmentation of the pseudoorbitals by diffuse and polarization (2 fg) functions as mentioned above [23]. Several implicit solvation models were applied together with this electronic level:

a) IEFPCM with 1.2 scaled UAHF radii (as it was default in Gaussian 03).
b) DPCM with the same cavities and charge compensation so that the outlying charge is accounted for by means of an additional effective charge, distributed according to the solute electronic density (keyword ICOMP=4 in G98 and G03).
c) DPCM with the scaled cavities (further labeled DPCM/sUAHF) and computational model as suggested in ref. [43].
d) COSMO (CPCM) with the original Klamt's radii.

For a comparison also SM8 Truhlar's model as implemented in GAMESSplus 2009 program [44, 45] was used with charge model 4 (CM4), the RADII5 option for cavity construction, and basis set 6-31++G(d,p). Two different functionals were chosen in the SM8 model:

e) M06 functional (including 0.27 fraction of the HF exchange energy).
f) MPWX functional - MPWX is a combination of the mPW exchange functional of Adamo and Barone [46], the $PW91$ correlation functional [47] and X means a percentage of HF exchange (in our case 25% was used according to the authors' recommendation).

For a more detailed description of the SM8 solvation model see ref. [48]. The set of solvent models is completed by:

g) COSMO-RS method as programmed in COSMOtherm C21-016 software [49–51].

The acidic dissociation constants (pK$_a$) of Eq. 2 were determined at all these a)-f) levels and used for the determination of equilibrium constants pK' of the hydration process from Eq. 1. In the case f) the COSMO-RS pK$_a$ constants were combined with the transformed Gibbs free energy $\Delta G'$ from the COSMO model.

In order to get suitable thermodynamic potential, which has pH as a natural variable, Legendre transformation of classical Gibbs free energy $dG = -S.dT + V.dp + \sum_i \mu_i.dn_i$ was done [52]:

$$G' = G - n(H)\mu(H^+), \tag{4}$$

where $\Delta G'^{\circ}$ is associated with equilibrium constant K' according to van't Hoff isotherm equation: $\Delta G'^{\circ} = -RT \ln K'$. In equilibrium, all 'proton chemical potentials' of the related species, which differ just by number of 'active' protons, must be the same. This condition can be mathematically rewritten in the form:

$$K' = \frac{(\sum [C])(\sum [D])}{(\sum [A])(\sum [B])} \qquad (5)$$

where each of the sums: $\sum [X]$ means all different forms of one of the reactants or products. In this way concentrations of all of these species appear in the equilibrium constant for the reaction under constant pH. For instance, regarding the first reaction in Eq. 1, the following equilibrium constant is obtained:

$$K' = \frac{\left[cis - [Pt(NH_3)_2Cl(H_2O)]^+\right] \cdot [Cl^-]}{[Pt(NH_3)_2Cl_2] \cdot [H_2O]} \times \frac{\left\{1 + \frac{K_A^{[Pt(NH_3)_2Cl(OH)]}}{[H^+]}\right\}}{\left\{1 + \frac{K_A^{(OH^-)}}{[H^+]} + \frac{[H^+]}{K_A^{(H_3O^+)}}\right\}}$$

$$(6)$$

(Eq. 3) supposing, e.g., the concentration of hydroxide anion can be determined from acidic dissociation constant of water: $[OH^-] = [H_2O]\frac{K_A^{(OH^-)}}{[H^+]}$. Having evaluated this K' for given pH, known pK_a, and quantum chemically calculated K (the first fraction term in Eq. 6), the transformed Gibbs potential can be determined.

In cellular solution, a constant concentration of [Cl⁻] should be considered, too. However, we do not need to consider simultaneous occurrence of such species due to their negligible probability. Constant Cl⁻ concentration will be considered through the modified standard reference state since $[Cl^-] \neq 1$ mol/dm³ in the same way like concentration of water in solution (55.5 mol/dm³).

pK$_a$ determination

First, the acidic dissociation constants for hydrated platinum complexes have to be determined. Since we are interested in the pH range from 0 to 14 we do not need to consider the protonation of Cl- to HCl ($pK_a \approx -6$) and deprotonation of NH₃ ligands ($pK_a \approx 18$–22) in cisplatin/transplatin complexes, because their influence on the K' values is negligible in this pH range (according to Henderson-Hasselbach equation).

The pK_a values were determined for the seven above-mentioned approaches and they are collected for both cisplatin and transplatin hydration reactions in Table 2. For comparison, also the pK_a of isolated ligands HCl, H₂O, and NH₃ (or its conjugated acid NH₄⁺) were determined. The calculations at CCSD(T) electronic level were also combined with one of the most successful models (DPCM/UAHF). Nevertheless this model is not superior to the B3LYP/DPCM/UAHF one. Practically all the calculated pK_a values at the CCSD)(T) level are worse than the B3LYP results, in comparison with experimental data. Note that even though CCSD(T) method is used, the solute-solvent interaction is described only at the Hartree-Fock level, because correlation effects are not included in the most implicit solvent models.

All pK_a estimations are based on the chemical equation: $HA + H_2O \rightarrow H_3O^+ + A^-$. Also, only for the best performing DPCM models another way of evaluation of acidic dissociation constants was used: $HA \rightarrow H^+ + A^-$. In this case, the fitted value of solvation free energy of proton is available from our previous study [43] where more comprehensive analysis of several PCM methods and several possibilities for cavity construction is presented. The fitted value of $\Delta G_{solv}(H^+) = -262.4$ kcal mol⁻¹ is in fair accord with recent measurement by Tissandier et al.

Table 2 Estimated pK$_a$ values by chosen computational model pK$_a$(c) labels cisplatin and pK$_a$(t) transplatin complexes from Eq. 2

	Exp	DPCM sUAHF H⁺ B3LYP	DPCM UAHF H⁺ B3LYP	DPCM UAHF H₃O⁺ B3LYP	DPCM UAHF H₃O⁺ CCSD	IEFPCM UAHF H₃O⁺ B3LYP	CPCM UAHF H₃O⁺ B3LYP	SM8 CM4 H₃O⁺ M06	SM8 CM4 H₃O⁺ MPWX	DPCM sUAHF H⁺ B3LYP
pK$_{a1}$(c)	6.6	6.6	8.0	6.4	7.5	6.7	20.0	9.0	6.7	4.7
pK$_{a21}$(c)	5.5	4.9	3.7	2.1	2.7	1.7	17.4	11.1	11.6	8.8
pK$_{a22}$(c)	7.3	7.8	9.6	8.0	9.1	8.3	21.7	8.8	12.4	9.9
pK$_{a1}$(t)	5.6	6.6	7.2	5.6	1.0	6.0	19.2	8.7	7.7	5.4
pK$_{a21}$(t)	4.4	4.9	0.3	−1.3	−6.6	−1.7	14.5	9.8	9.9	6.8
pK$_{a22}$(t)	7.3	8.4	11.1	9.5	12.0	9.8	22.6	9.4	17.1	14.3
pK$_a$(HCl)	−6.1	−7.1	−6.7	−8.3	−5.0	−6.0	8.8	−6.6	−8.1	−9.5
Kv	15.4	16.1	15.9	15.9	18.5	19.7	19.7	15.0	20.2	16.6
pK$_a$(NH₄⁺)	9.2	7.7	8.7	7.1	6.9	6.5	23.4	13.1	23.4	27.5
RMSD		1.4	2.2	2.6	4.6	3.1	13.2	4.6	4.9	3.1

[53]: $\Delta G_{solv}(H^+) = -264.0$ kcal mol^{-1}. These sets of pK$_a$ display the smallest RMS difference from experimental values presented in Table 2 (1.41 and 2.24). The second value is quite close to the approach based on the same DPCM/UAHF model with hydronium cation (2.55). The IEFPCM and SM8 (with MPWX functional) approaches are also relatively accurate (RMSD=3.1). Determination of the pK$_{a21}$ values requires energies of solvated bivalent Pt (II) cations, which is a difficult task for models with non-scaled cavities. Here the superiority of the model with scaled cavities is clearly demonstrated (see also Dupuis's studies on this topic [54–56]).

When comparing the individual pK$_a$ values it can be noticed that the most problematic systems are dications of diaqua-platinum, which are determined relatively inaccurately. This has serious consequences in further determination of hydration equilibrium constants as will be shown in the next part. Not surprisingly, also the pK$_a$ value of the NH$_4^+$ cation deviates from experimental data by more than two log units in most models, since amines in general represents a difficult case for implicit solvation models. The biggest differences between calculated and experimental values were obtained with the CPCM model. As for COSMO-RS, the pK$_a$ values were obtained using the default settings of the COSMOtherm program.

Constant-pH model

Having determined pK$_a$ values, the transformed $\Delta G'$ energies can be evaluated according to Eq. 6. First, the values of the regular free energies ΔG were calculated and corresponding equilibrium constants K were estimated. The values obtained for the selected computational models are collected in Table 3. Comparing the values collected for cisplatin and transplatin complexes, it can be noticed that all the models agree with the experiment at least in the fact that systematically higher pK's were obtained for transplatin in comparison with cisplatin. Nevertheless, the experimental values of pK were obtained under the constant pH condition (at pH=7.4). From this point of view they should not be directly compared with the values in Table 3 since they correspond to different thermodynamic potential ($\Delta G'$ and ΔG, respectively), as mentioned in the introduction. In order to do the proper comparison, the Legendre transformed Gibbs free energies $\Delta G'$ should be used. The transformed equilibrium constants K' for the hydration processes are displayed in the pH ranging from 0 to 14 in Fig. 1. The role of pK$_a$'s clearly follows from the figure. According to Henderson-Hasselbach equation the slope of the pK curve rapidly changes where pH equals pK$_a$ of some of involved species, for instance, in Fig. 1a when monoaqua-cisplatin undergoes deprotonation to the monohydroxo-cisplatin complex. In Fig. 1b and d, a more complex situation can be seen since all three pK$_a$ constants influence the pK curves. Similarly to the previous part much better performance of the model with scaled cavities can be noticed in the pK values, which concern calculations of DDP_2w (bivalent cations of diaqua-cis/trans-platin complexes) where much lower values (up to 6 logarithmic units) were obtained.

In all the plots, the experimentally determined equilibrium constant for pH=7.4 is drawn as a rhomb sign. Comparing all studied solvation models, the DPCM/sUAHF approach performs excellently. RMSD for four pK values at pH=7.4 is 0.93 at this level while the second most successful model (based on non-scaled cavities: DPCM/UAHF and H$_3$O$^+$) already has the RMSD at about

Table 3 Equilibrium constants (pK) for cis/trans-platin hydration process

	Exp	DPCM sUAHF H$^+$ B3LYP	DPCM UAHF H$^+$ B3LYP	DPCM UAHF H$_3$O$^+$ B3LYP	DPCM UAHF H$_3$O$^+$ CCSD	IEFPCM UAHF H$_3$O$^+$ B3LYP	CPCM UAHF H$_3$O$^+$ B3LYP	SM8 CM4 H$_3$O$^+$ M06
cDDP->cDDP_w	5.2	5.9	5.9	8.8	8.6	9.9	2.6	2.1
cDDP->cDDP_h	11.8	13.9	12.3	16.3	15.2	29.9	9.2	6.7
cDDP_w–>cDDP_2w	6.8	9.3	9.3	12.9	12.5	11.2	−4.8	−5.4
cDDP_w–>cDDP_hw	11.7	13.0	11.4	15.6	14.1	28.5	6.7	3.3
cDDP_h–>cDDP_hw	6.0	5.0	5.0	8.1	7.4	8.5	0.1	−1.3
cDDP_h–>cDDP_2h	13.0	14.6	13.0	17.2	15.7	30.2	12.5	8.6
tDDP->tDDP_w	7.0	8.7	8.7	23.0	11.1	11.5	8.6	7.6
tDDP->tDDP_h	13.6	15.9	14.4	24.1	17.1	30.7	16.3	13.0
tDDP_w–>tDDP_2w	6.8	12.5	12.5	27.3	15.7	14.1	−2.3	−2.2
tDDP_w–>tDDP_hw	11.7	12.8	11.2	20.7	14.0	28.6	7.7	4.7
tDDP_h–>tDDP_hw	7.1	5.6	5.6	19.7	8.0	9.4	0.0	−0.7
tDDP_h–>tDDP_2h	13.5	16.7	15.1	26.0	17.9	32.0	17.1	13.5

2.6. The DPCM/(s)UAHF and SM8/MPWX models agree relatively reasonably with measured data especially for the first hydration step where only neutral and monovalent complexes are calculated.

Finally, the plots of equilibrium molar fractions of individual chemical species originated from the dissolved cisplatin/transplatin complexes in water solution with dependence on pH are compared to the experimental curves in the Martin's study [4], which were obtained in solution with 4 mM concentration of chloride anions. Also the corrections to the reference state based on the given chloride concentration in water solution (with 55.5 molar concentration of water) was taken into account in our calculations.

In Fig. 2 a)-d), the comparison of the molar fractions of the three (most successful) solvation models with experimental data is displayed for the cisplatin complex. At first glance fair agreement of the SM8 method with experimental molar fraction in acidic pH range can be noticed. However, concentration of hydroxo-cisplatin quickly increases and become too dominant around pH=7. Therefore, the SM8 model predicts no real activation for pH>5. The hydroxo-cisplatin complex is too stable and prevents the further substitution reaction of this ligand. As to cisplatin activation, better results are obtained with the DPCM model where hydroxo-aqua-cisplatin complex prevails in the neutral pH range, despite the fact that its concentration is still a little higher. This is a consequence of the shifted equilibrium constant (pK_1=2.6 comparing 2.2 value at pH=7.4) for the first hydration step. This model also, correctly 'predicts' dominant occurrence of the dihydroxo-complex in basic solutions.

In the case of the transplatin complex, analogous plots are drawn in Fig. 2 e)-h). It is evident that transplatin is visibly less activated than cisplatin, which means that much lower concentration of aqua-form is present in acidic and neutral solutions. However, this situation is not correctly reproduced by any of the chosen solvation models. In the SM8 model, too high value of pK_{22} is responsible for dominant hydroxo-aqua-complex in basic environment since only after pH=13 dihydroxo-form starts to prevail. From this point much better performance was obtained by both PCM approaches. It can be seen that the best method (DPCM/sUAHF) is able to reproduce at least some concentration of the monochloro-monohydroxo- and mono-aqua-monohydroxo-transplatin complex around pH=8.

The effect of chloride concentration on the molar fractions of individual form of cisplatin is shown in

Fig. 1 The dependence of the pK for the hydration process of the platinum complex on the pH of the solution (axes). (a) first step of the hydration reaction of cisplatin. (b) second hydration step of cisplatin. (c) first step of the hydration process of transplatin. (d) second hydration step of transplatin
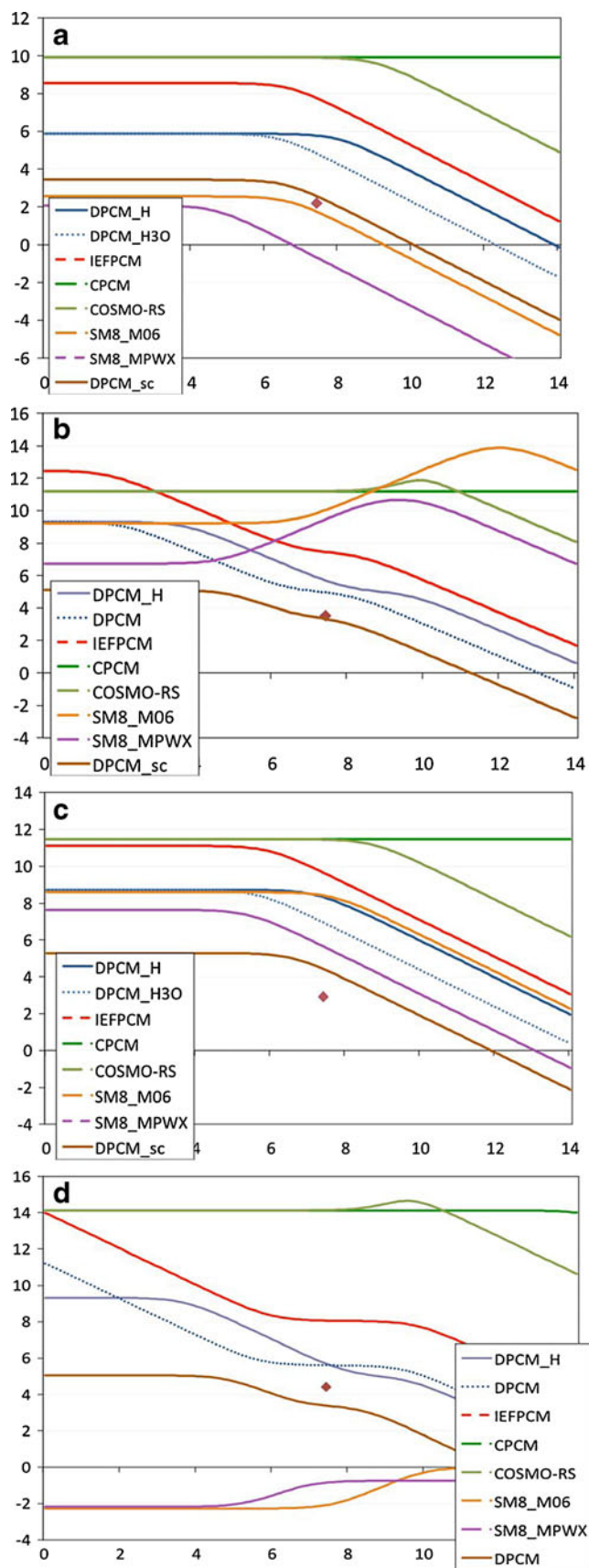
Fig. 2 Comparison of various solvation models for the dependence of the molar fractions of platinum (II) complexes on pH of the solutions with 4 mM concentration of dissolved cisplatin complex. (**a**) and (**e**) experimental values; (**b**) and (**f**) DPCM; (**c**) and (**g**) IEFPCM; (**d**) and (**h**) SM8/MPWX
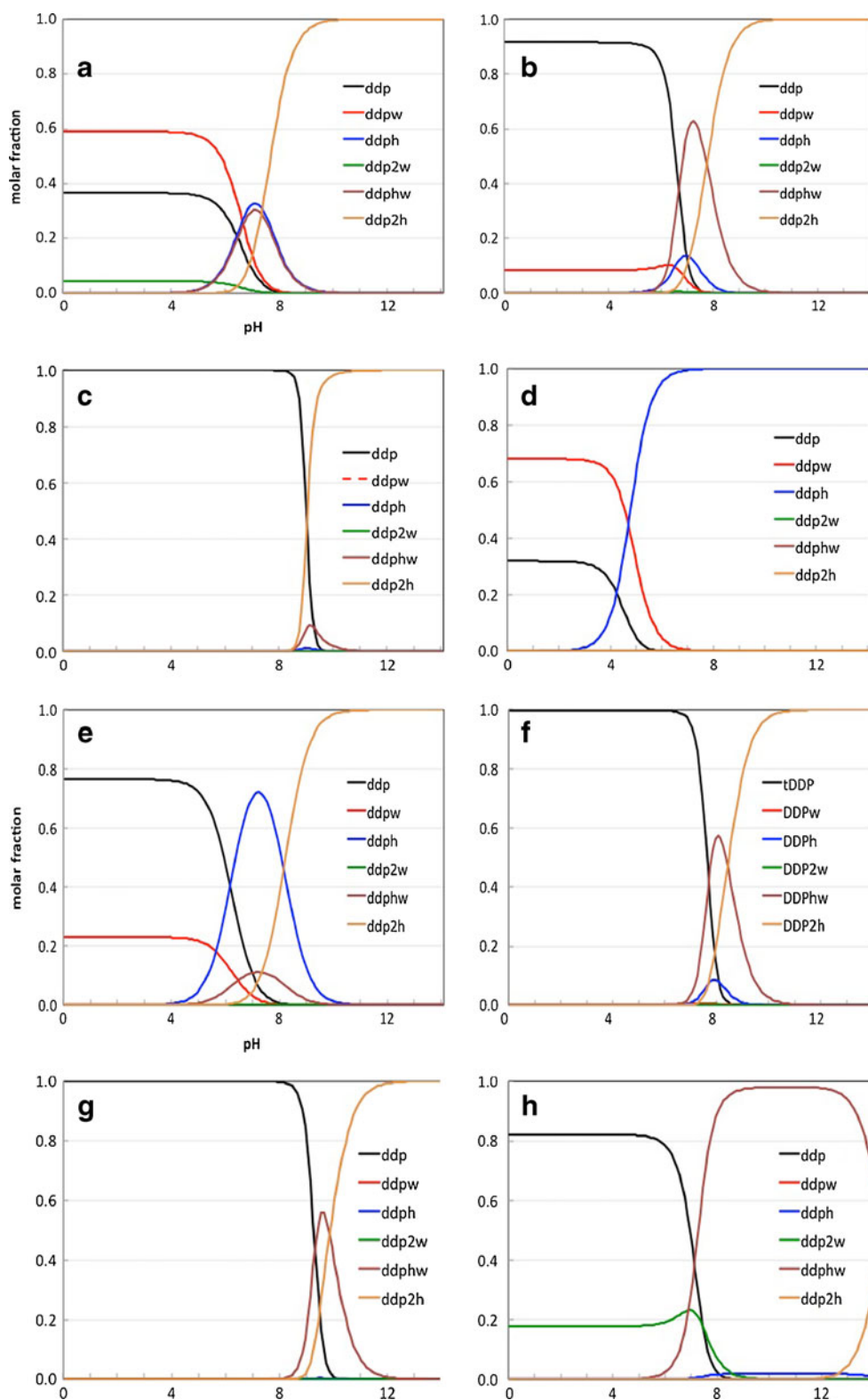

Fig. 3. Comparing experimental curves, lower molar fraction of both active aqua-complexes can be seen in plot c). Similar lowering is also apparent, at least qualitatively, comparing plot b) and d) for aqua- and hydroxo-aqua-complexes.

Conclusions

This study describes the thermodynamics of the hydration process of cisplatin and transplatin under the model of constant pH. Several implicit solvation models were

Fig. 3 The influence of the chloride concentration on the molar fraction of active (aqua) platinum complexes. (a) and (c) experimental values; (b) and(d) DPCM; (a) and (b) 4 mM concentration of Cl anions; (c) and (d) 104 mM concentration of Cl⁻
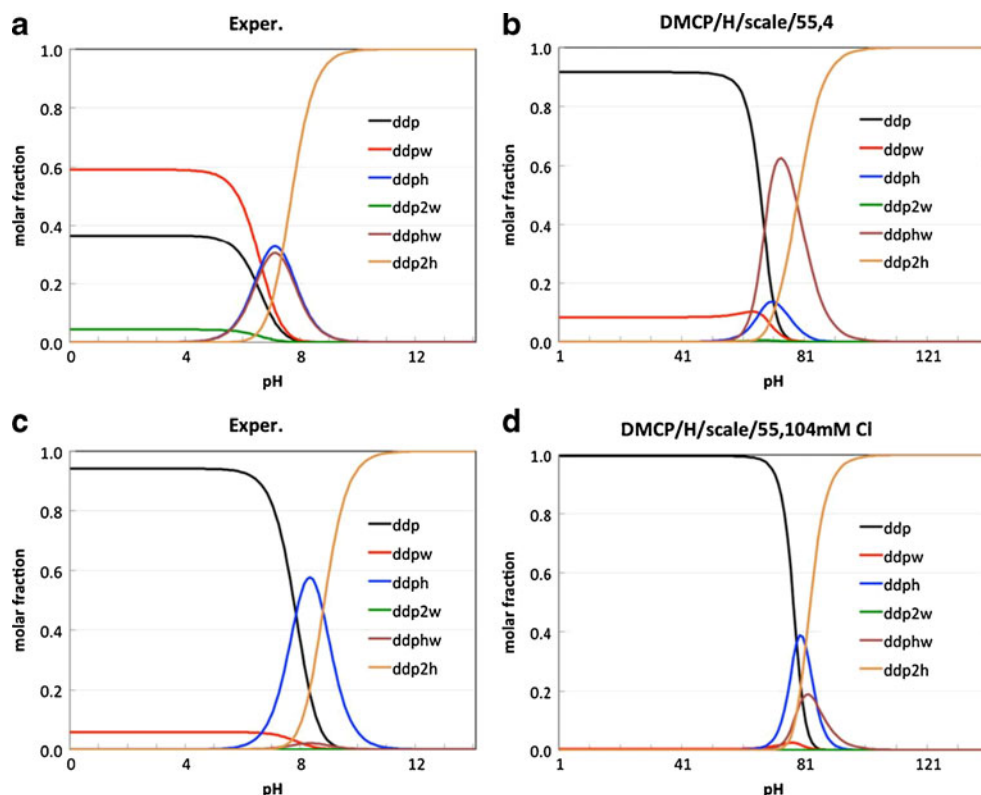
compared based on the pK$_a$ acidic dissociation constants and standard pK constant for the hydration reactions of the platinum(II) complexes. Three basic variants of the PCM model available in Gaussian 03 program (DPCM, IEFPCM, and CPCM) were combined with the B3LYP functional and the UAHF method for cavity construction and compared with the COSMO-RS (in program COSMOtherm) and SM8 model developed by Truhlar. Two different DFT functionals (M06 and MPWX) and charge model CM4 (as implemented in program GAMESSplus 2009) were applied with the SM8 model.

The RMS difference between experimental and calculated pK$_a$ values of cis/transplatin, water, HCl, and NH$_4^+$ was used as an accuracy criterion. In accord with our previous study [43] (where SM8 models were not included) the DPCM approach was confirmed as the most accurate (despite the fact that a lot of space is still available for further improvement). The pK$_a$ constants were used in Legendre transformation to determine the ΔG' energies and K' equilibrium constants in the solution with constant pH. Figure 1, shows that similarly to the calculation of the pK$_a$ constants, the DPCM, IEFPCM, and SM8/MPWX models are the most successful in estimation of pK', even though the agreement with experiment is rather qualitative for non-scaled models.

The influence of low cellular Cl⁻ concentration was demonstrated for the DPCM model. In accord with experimental results, the increased ratio of cisplatin active aqua-forms can be noticed for 4 mM chloride solutions (cellular nucleus) in comparison with 104 mM environment (in the extracellular fluid).

References

1. Hindmarsh K, House DA, Turnbull MM (1997) Inorg Chim Acta 257:11–18
2. Arpalahti J, Mikola M, Mauristo S (1993) Inorg Chem 32:3327–3333
3. Mikola M, Arpalahti J (1994) Inorg Chem 33:4439–4445
4. Martin RB (1999) In: Lippert B (ed) Cisplatin. Wiley-VCH, Weinheim, pp 183–206
5. Berners-Price SJ, Frenkiel TA, Frey U, Randolf JD, Sadler PJ (1992) J Chem Soc Chem Commun789-795
6. Orton DM, Gretton VA, Green M (1993) Inorg Chim Acta 204:265–278
7. Appleton TG, Bailey AJ, Barnham KJ, Hall JR (1992) Inorg Chem 31:3077–3091
8. Mikola M, Arpalahti J (1996) Inorg Chem 35:7556–7564
9. Lippert B (1999) Cisplatin: Chem. and Biochemistry of a leading anticancer drug. Wiley-VCH, Weinheim, Germany
10. Wilkins RG (1991) Kinetics and mechanism of reactions of transition metal complexes. Wiley-VCH, Weinheim
11. Chval Z, Sip M, Burda JV (2008) J Comput Chem 29:2370–2381

12. Schmuelling M, Lippert B, van Eldik R (1994) Inorg Chem 33:3276–3282
13. Bradáč O, Zimmermann T, Burda J (2008) J Mol Model 14:705–716
14. Bancroft DP, Lepre CA, Lippard SJ (1990) J Am Chem Soc 112:6860–6867
15. Bernges F, Doerner G, Holler E (1990) Eur J Biochem 191:743–747
16. Bernges F, Holler E (1991) Nucleic Acids Res 19:1483–1498
17. Arpalahti J (1996) In: Sigel ASH (ed) Metal Ions in Biological Systems. Dekker, New York, p 380–395
18. Jestin JL, Lambert B, Chottard JC (1998) J Biol Inorg Chem 3:515–519
19. Mudroch P del S, Guo Z, Parkinson JA, Sadler PJ (1999) J Biol Inorg Chem 4:32–38
20. Lemma K, Shi T, Elding LI (2000) Inorg Chem 39:1728–1734
21. Burda JV, Zeizinger M, Leszczynski J (2004) J Chem Phys 120:253–1262
22. Burda JV, Zeizinger M, Leszczynski J (2005) J Comput Chem 29:907–914
23. Burda JV, Zeizinger M, Šponer J, Leszczynski J (2000) J Chem Phys 113:2224–2232
24. Zeizinger N, Burda JV, Sponer J, Kapsa V, Leszczynski J (2001) J Phys Chem A 105:8086–8092
25. Zhang Y, Guo Z, You XZ (2001) J Am Chem Soc 123:9378–9387
26. Robertazzi A, Platts JA (2004) J Comput Chem 25:1060–1067
27. Costa LAS, Rocha WR, De Almeida WB, Dos Santos HF (2004) Chem Phys Lett 387:182–187
28. Costa LAS, Rocha WR, De Almeida WB, Dos Santos HF (2003) J Chem Phys 118:10584–10592
29. Lopes JF, Menezes VSD, Duarte HA, Rocha WR, De Almeida WB, Dos Santos HF (2006) J Phys Chem B 110:12047–12054
30. Lopes JF, Rocha WR, Dos Santos HF, De Almeida WB (2008) J Chem Phys 128:165103
31. Lopes JF, Rocha WR, dos Santos HF, de Almeida WB (2010) J Braz Chem Soc 21:887–896
32. Chojnacki H, Kuduk-Jaworska J, Jaroszewicz I, Janski JJ (2009) Pol J Chem 83:1013–1024
33. Fu CF, Tian SX (2010) J Chem Phys 132: 174507
34. Banerjee S, Sengupta PS, Mukherjee AK (2010) Chem Phys Lett 497:142–148
35. Lucas MFA, Pavelka M, Alberto ME, Russo N (2009) J Phys Chem B 113:831–838
36. Pavelka M, Lucas MFA, Russo N (2007) Chem Eur J 13:10108–10116
37. Beret EC, Pappalardo RR, Marx D, Marcos ES (2009) Chem Phys Chem 10:1044–1052
38. Dans PD, Coitino EL (2009) J Chem Inf Model 49:1407–1419
39. Cossi M, Rega N, Scalmani G, Barone V (2003) J Comput Chem 24:669–681
40. Barone V, Cossi M (1998) J Phys Chem A 102:1995–2001
41. Andrae D, Haussermann U, Dolg M, Stoll H, Preuss H (1990) Theor Chim Acta 77:123–141
42. Bergner A, Dolg M, Kuechle W, Stoll H, Preuss H (1993) Mol Phys 80:1431–1447
43. Zimmermann T, Burda JV (2009) J Chem Phys 131:135101
44. Higashi M, Marenich AV, Olson RM, Chamberlin AC, Pu J, Kelly CP, Thompson JD, Xidos JD, Li J, Zhu T, Hawkins GD, Chuang Y-Y, Fast PL, Lynch BJ, Liotard DA, Rinaldi D, Gao J, Cramer CJ, Truhlar DG (2009) GAMESSPLUS, version 2009. University of Minnesota, Minneapolis
45. Schmidt MW, Baldridge KK, Boatz JA, Elbert ST, Gordon MS, Jensen JH, Koseki S, Matsunaga N, Nguyen KA, Su SJ, Windus TL, Dupuis M, Montgomery JA (1993) J Comput Chem 14:1347–1361
46. Adamo C, Barone V (1998) J Chem Phys 108:66–82
47. Perdew JP (1991) In: Zieesche P, Eshrig H (eds) Electronic Structure of Solids. Akademie, Berlin
48. Marenich AV, Olson RM, Kelly CP, Cramer CJ, Truhlar DG (2007) J Chem Theory Comput 3:2011–2019
49. Klamt A, Schuurmann G (1993) J Chem Soc Perkin Trans 2799–2805
50. Klamt A (1998) In: Schleyer PvR (ed) Encyclopedia Computational Chemistry. Wiley, Chichester
51. Klamt A, Eckert F, Hornig M, Beck ME, Burger T (2002) J Comput Chem 23:275–281
52. Alberty RA (2001) Pure Appl Chem 73:1349–1380
53. Tissandier MD, Cowen KA, Feng WY, Gundlach E, Cohen MH, Earhart AD, Coe JV, Tuttle TR (1998) J Phys Chem A 102:7787–7794
54. Ginovska B, Camaioni DM, Dupuis M (2007) J Chem Phys 127:084309
55. Ginovska B, Camaioni DM, Dupuis M (2008) J Chem Phys 129:014506
56. Ginovska B, Camaioni DM, Dupuis M, Schwerdtfeger CA, Gil QJ (2008)Phys Chem A 112:10604–10613